



SolarPACES 2013

## Corrosion of iron stainless steels in molten nitrate salt

Alan Kruiuzenga<sup>a</sup>, David Gill<sup>b</sup>

<sup>a</sup> Sandia National Laboratories, P.O.Box 969, Livermore CA 94551, USA

<sup>b</sup> Sandia National Laboratories, P.O.Box 5800, Albuquerque NM 87185, USA

---

### Abstract

Energy storage for concentrating solar power (CSP) is a major area of research that seeks to lower the levelized cost of electricity within the aggressive SunShot goals of 6¢/kW-hr<sub>th</sub>[1-3]. One viable approach is sensible thermal energy storage (TES), which currently utilizes molten nitrate binary salt, stored at 575°C in the hot tank of a two tank system [4, 5]. Increasing the temperature limit within the hot tank requires a detailed understanding of materials corrosion behavior, in addition to salt thermal stability properties.

High temperature nickel based alloys are the logical choice for strength and corrosion resistance as elevated temperatures will increase corrosion kinetics, however, the cost of nickel based alloys are nearly four times more expensive than iron based steels [6]. For this reason iron based stainless steels, specifically 321SS and 347SS (nominally Fe-17Cr-9Ni), were chosen for investigation at several temperatures in nitrate salt. 316SS, an elementally similar alloy, was susceptible to stress corrosion cracking while tested at Solar Two [4]. It was suggested that alloys with stabilizing additions of niobium (347SS) or titanium (321SS) would mitigate this deleterious behavior.

Flat coupon samples were immersed in binary nitrate salts at temperatures of 400, 500, 600, and 680°C, with air sparging on all tests. Samples were nominally removed at intervals of 500, 1000, 2000, and 3000 hours to acquire data on time varying weight gain information while simultaneously employing metallography to identify corrosion mechanisms occurring within the melt.

Corrosion rates varied dramatically with temperature according to an Arrhenius-type behavior. 347SS and 321SS had very little oxidation for 400 and 500°C, indicative of a protective corrosion scale and low corrosion kinetics. Data at 600°C showed that 321SS tended toward linear oxidation behavior based on oxide spallation which was observed on the samples upon removal.

Corrosion products at 500°C had phases of iron oxide, with obvious chromium depletion as observed in energy dispersive spectroscopy (EDS) scans. 600°C corrosion layers were primarily iron oxide with obvious phases of sodium ferrite on the outer surface. 680°C marked an excessive rate of corrosion with metal loss in both alloys.

Published by Elsevier Ltd. This is an open access article under the CC BY-NC-ND license (<http://creativecommons.org/licenses/by-nc-nd/3.0/>).

Selection and peer review by the scientific conference committee of SolarPACES 2013 under responsibility of PSE AG.

Final manuscript published as received without editorial corrections.

**Keywords:** Austenitic Steel, Molten Nitrate Salt, High Temperature Corrosion

---

## 1. Introduction

Increasing the maximum operating temperature of power cycles results in higher efficiency power plant operation[7]. Material stability and performance at high temperatures are of one major limitation in increasing this operating temperature, particularly when considering thermal energy storage (TES) and receiver systems. Currently two tank TES systems operate with the hot tank at 565°C [5] and the cold tank operating at 290°C[4]. The cold tank on Solar Two was built of carbon steel (ASTM A516-70), while the hot tank and receiver required use of stainless steel; 304SS and 316SS.

304SS and 316SS are both similar in that they are nominally Fe-18Cr-10Ni (by weight) alloy. 316SS has additions of molybdenum to promote corrosion resistance. During testing at Solar Two, concerns regarding stress corrosion cracking (SCC) following an aqueous rinse of the receiver led to studies investigating structural materials that have better resistance to SCC and intergranular corrosion (IGC).

IGC in stainless steels are caused by exposure to temperature conditions favoring formation of chromium carbide at grain boundaries[8]. Since the formation of chromium carbide depletes chromium at the grain boundaries this creates a situation in which an alloy is sensitized to corrosion along the chromium depleted regions. Materials that may mitigate sensitization have elemental additions to stabilize the alloys.

Two iron based alloys were investigated for this reason. 347SS and 321SS have similar composition, as illustrated in Table 1, but are stabilized by titanium (321SS) or niobium (347SS). Corrosion experiments were performed over four temperature ranges (400, 500, 600 and 680°C) and up to 3000 hours in duration. The purpose of this test is to provide initial data on relative performance between these alloys and to determine changes in corrosion mechanisms as a function of temperature.

<b>Nomenclature</b>	
BEI	Backscatter Electron Image
CSP	Concentration Solar Power
EDS	Energy Dispersive Spectroscopy
EMP	Electron Microprobe
IGC	Intergranular corrosion
NSTTF	National Solar Thermal Test Facility
SCC	Stress corrosion cracking
SEI	Secondary Electron Image
SEM	Scanning Electron Microscope/Microscopy
SNL	Sandia National Laboratories
TES	Thermal Energy Storage
XRD	X-ray Diffraction

## 2. Procedures

Static immersion tests were performed at the National Solar Thermal Test Facility (NSTTF) located at Sandia National Laboratories in Albuquerque New Mexico[9]. Results presented here are a subset of a larger array of alloys tested [10]. Exposures were performed at four temperatures, which were chosen to reflect different operating conditions within a CSP plant, such as the hot and cold storage tanks, power block and solar receiver.

Test samples were mounted on sample trees and separated by ceramic beads, then immersed in the binary solar salt at a given temperature. Air was sparged through a cross drilled tube to provide mixing of the salt and ensure

that the partial pressure of O<sub>2</sub> was consistent throughout the course of the experiments, for the sake of salt chemistry through the nitrate/nitrite equilibrium.

Specimens were obtained from Metal Samples Company as 2”x1”x0.062” coupons with a 120 grit finish. Coupon removal was done nominally at 500, 1000, 2000, and 3000 hours. Weight gain and descaled data were determined from this data with guidance from ASTM standards [11]. Corrosion rates were calculated as follows [8]:

$$\frac{\mu\text{m}}{\text{yr}} = \frac{87600(\Delta M)}{\rho\tau} \quad (1)$$

$\Delta M$  is descaled mass loss per area (mg/cm<sup>2</sup>),  $\rho$  density of the alloy (g/cm<sup>3</sup>), and  $\tau$  is exposure time (hours). Four time steps were taking during most experiments due to space constraints [10]. Metal loss results were reported from the longest duration exposure time, which was a nominal 3000 hours for 400, 500, and 600°C. 680°C had an exposure of 1025 hours due to experimental concerns over excessive vessel corrosion.

Microscopy was employed to determine relevant corrosion reactions that occurred during exposures. Scanning electron microscopes (JEOL JSM 840A) equipped with energy dispersive spectroscopic systems (Thermo Electron Corp) were used. Images were generated correlating the presence of an element within a given area. The relative amount of an element present is related to image contrast; dark maps indicate little to none of the elemental species present, while bright maps correspond to high elemental concentration. Electron microprobe (EMP) was also employed to gain quantitative concentration data as a function of location.

X-ray diffraction (XRD) (PANalytical Empyrean) in 2 $\theta$  and goniometer modes was used on alloys with thick oxides and allowed for determination of surface corrosion phase. Alloys with thin or less-dense corrosion products, such as hematite or magnetite, proved more difficult to measure.

Table 1: Alloy composition used during corrosion tests.

Alloy	Cr	Mo	Ni	Mn	Si	Fe	Other
321SS†	17.28	0.34	9.10	1.80	0.63	70.37	Cu (0.32), Ti (0.16)
347SS†	17.45	0.32	9.43	1.57	0.63	69.72	Nb (0.62 max), Cu (0.26 max)

†actual composition tested from heat

### 3. Results

Corrosion performance of the stainless steels varied dramatically with temperature as shown in Table 2. Observed corrosion rates of 347SS were found to be consistently lower in comparison to 321SS by 40-50% at temperatures of 600°C and below, whereas at 680°C both alloys had effectively the same corrosion rate. Table 2 provides an indication of corrosion resistance for a given alloy and exposure condition.

Authors wholly acknowledge that system considerations ultimately govern whether a material is acceptable, but generally at or below 600°C alloys were found to have outstanding corrosion performance [8], with overall rates less than 25 $\mu\text{m}/\text{year}$ . However, tests at the high temperature can be considered good to fair; as good performance is typically regarded as metal loss of 100-500  $\mu\text{m}/\text{year}$  [8]. No indication of oxidation kinetics was found from this test (i.e. linear vs. parabolic), thus rates reported have used the more conservative linear kinetics in metal loss estimations.

An illustrative example of this considers 347SS exposed to salt for 30 years at 680°C. Calculations would predict 13.4mm of metal loss using linear oxidation kinetics. Readers should use extreme caution in making such long term extrapolations as uncertainties will vary significantly upon salt chemistry.

Table 2: Corrosion Rates and mass loss for iron based alloys

Alloy and Condition	Alloy Density [g/cm <sup>3</sup> ]	Descaled Loss [mg/cm <sup>2</sup> ]	Metal Loss [μm/year]
321SS	7.94		
400°C <sup>a</sup>		0.27	1
500°C <sup>a</sup>		1.98	7.1
600°C <sup>b</sup>			15.9
680°C <sup>c</sup>		42.77	460
347SS	8.03		
400°C <sup>a</sup>		0.2	0.7
500°C <sup>a</sup>		1.28	4.6
600°C <sup>b</sup>		-	10.4
680°C <sup>c</sup>		42.05	447

a. Based on 3064 hour exposure using equation 1  
 b. Data from Reference [10] after 3000 hours  
 c. Based on 1025 hour exposure using equation 1

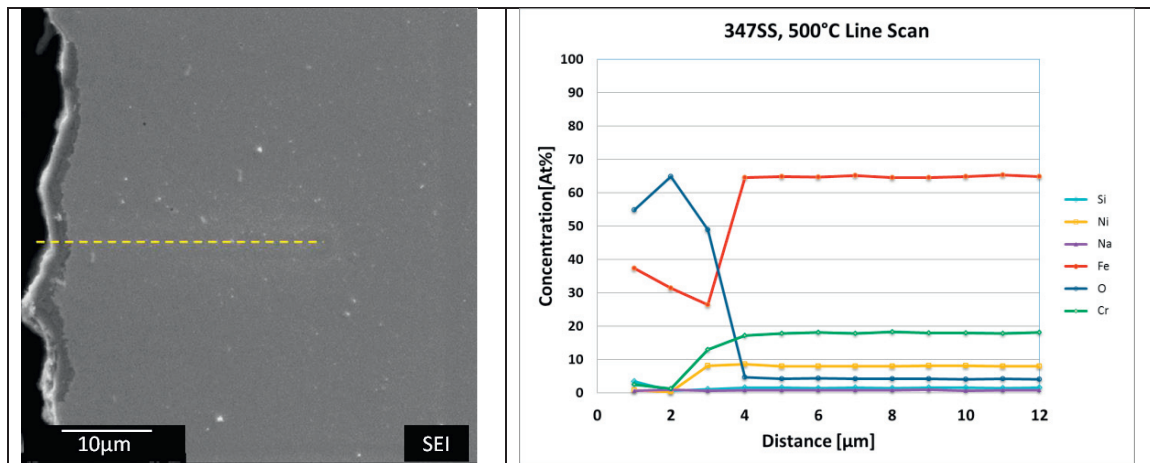


Figure 1: 347SS after 3064 hours at 500°C with iron oxide found as the primary surface product

Microscopy and other metallographic examinations were employed to provide insight into changing mechanisms and corrosion morphologies as a function of temperature. SEM was primarily used with cross section views to determine depth of attack and corrosion structure. As expected, from corrosion rate data, oxidation scales on both alloys at 400°C was minimal. No useful information could be extracted from tests of this temperature condition. Corrosion scales on alloys exposed at 500°C had thin scales, but could be characterized.

EMP scans of alloys exposed at 500°C (Figure 1 and 2) indicate scales ranged in thickness, but were found to be nominally 4-8μm thick. Oxides were chromium depleted as observed in past studies [12-14]. Chromium depletion

is a direct result of the formation of soluble corrosion products within the melt, typically thought to be in the form of metal chromates [15]. Nitrate salts were tested for metals present in the melt and found that chromium was present in concentrations of approximately 50 ppm, further confirming solubility.

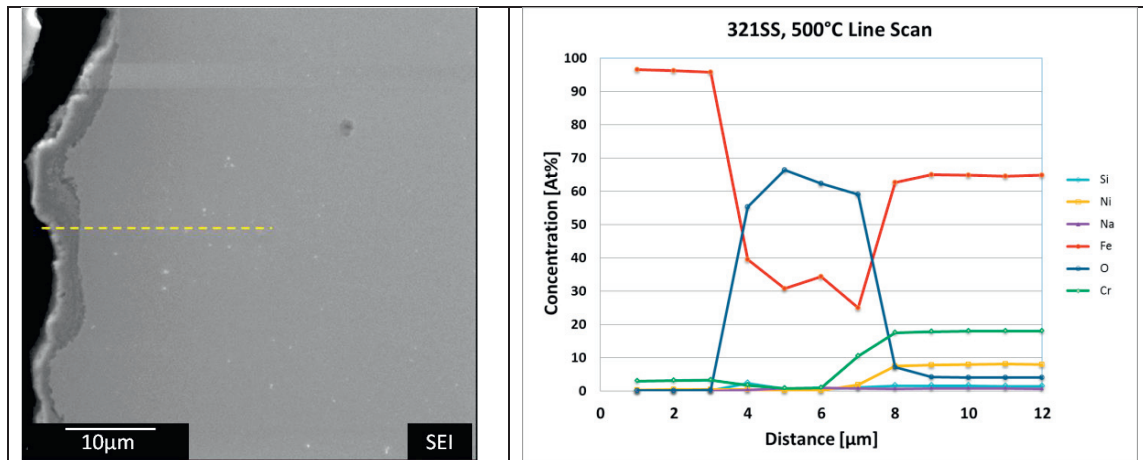


Figure 2: 321SS after 3064 hours exposure at 500°C.

As evidenced in EMP scans there was some variability in the oxidation layer with the outer most of the oxide being primarily iron oxide, either phases of  $Fe_2O_3$  or  $Fe_3O_4$ , transitioning to mixed oxides of iron, chromium, and possibly nickel. XRD information indicated that  $Fe_3O_4$  was the phase present on the surface. The only element from the nitrate salt participating in surface reaction was observed to be oxygen, as no sodium or potassium were observed at this temperature.

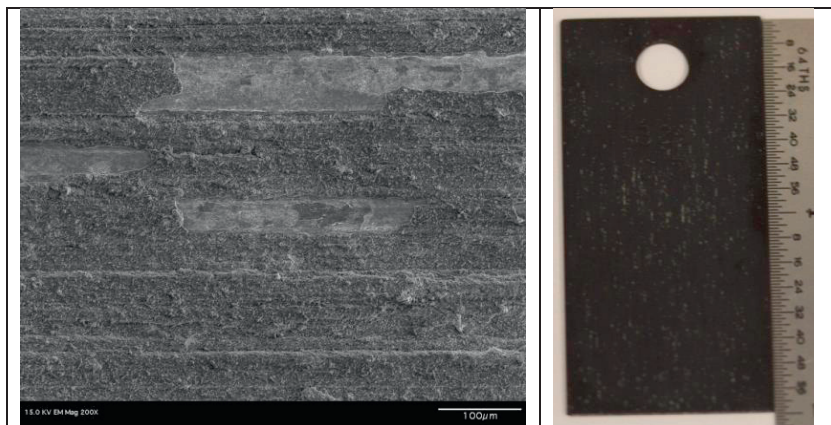


Figure 3: Plan view of 321SS after at 600°C for 1000 hours (top left image). Observed scaling present in photograph (top right) allowed for visual traces of spallation.

Alloys exposed to molten salts at 600°C had corrosion rates of approximately twice that observed for 500°C. Because reaction kinetics typically exhibit an Arrhenius relationship, this result was not particularly enlightening. However, several other key differences were noted.

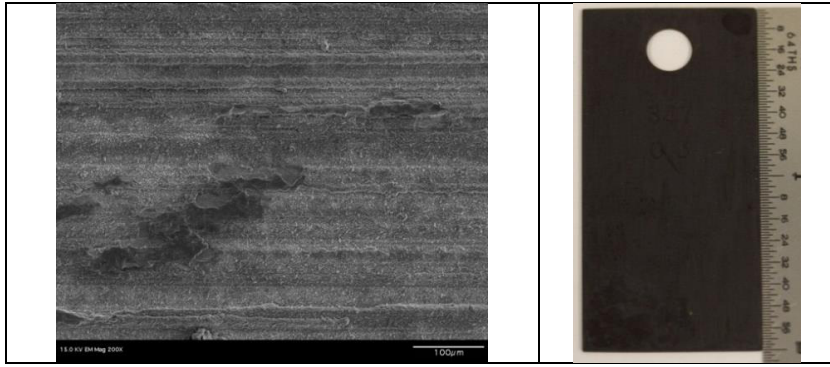


Figure 4: 600°C exposure of 347SS for nearly 3000 hours. No indication of spallation was observed.

First, surface spallation was observed on 321SS (Figure 3), while no obvious signs were present in 347SS (Figure 4). 321SS surface oxide exhibited poor adhesion in general, as flaking occurred during typical handling. Spallation was reported at higher temperatures (800-1000°) in oxygen environments, where studies found that oxides tended to spall upon cooling, due to stresses arising from the CTE mismatch of the alloy and oxides and are thought to apply to these observations [16] which may be of concern in regards to the diurnal thermal transients experienced in CSP plant operation.

Another observed difference was in corrosion products present on the surface. It was found through both EMP and XRD that sodium was present in the oxidation products in the phase of  $\text{NaFeO}_2$ . This is typical for high temperature ferrous alloys in sodium nitrate, but was generally expected to occur at temperatures above 600°C [17]. It is thought that this scale provides little to no base metal protection, as scale was easily removed by lightly sanding the surface.

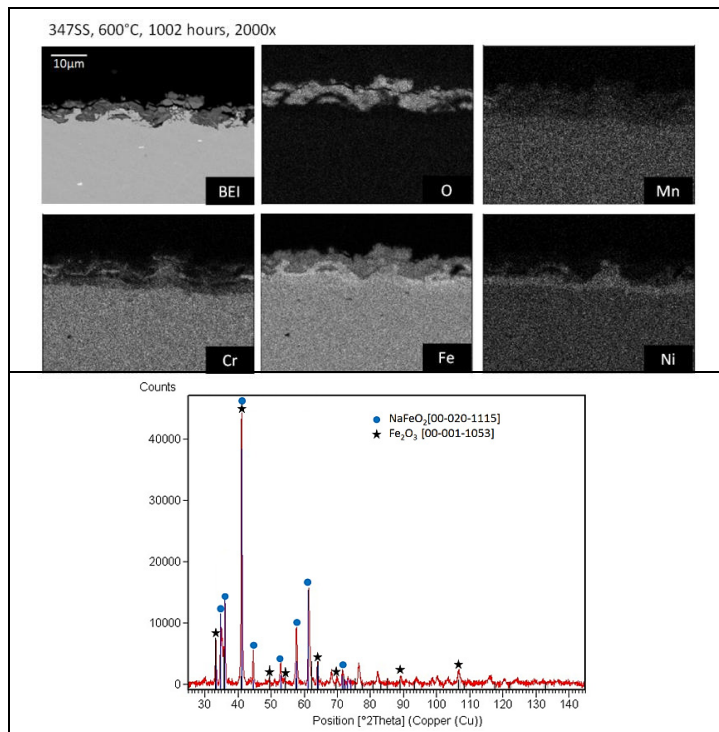


Figure 5: EDS map (top) and XRD data (bottom) for 347SS exposed at 600°C

Corrosion products beneath the sodium ferrite layer were identified to be primarily hematite, as shown in Figure 5. Line scan analysis, Figure 6, shows an oxide layer approximately 15 $\mu\text{m}$  thick. Mixed phases of hematite and sodium ferrite are both present in the first 8 $\mu\text{m}$  into the corrosion scale, while the hematite transitions into mixed phases of iron and chromium oxides around 10 $\mu\text{m}$ . Slight nickel enrichment was observed near the oxidation interface and is thought to be the result of the depletion of chromium from the bulk.

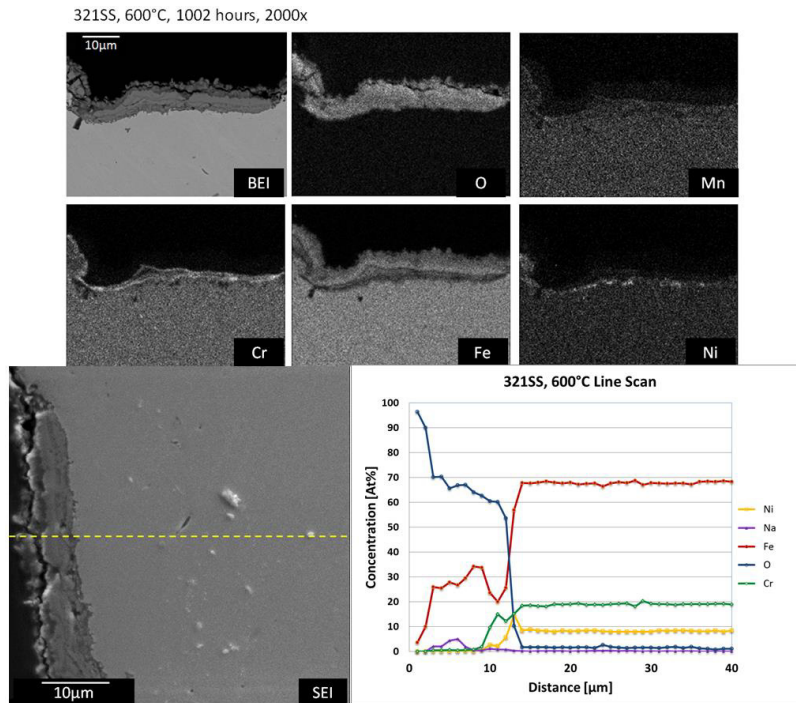


Figure 6: Cross sectional EDS mapping of 321SS with EMP line scan data. The formation of a duplex structure is observed, with outer layer of  $\text{NaFeO}_2$  and iron oxide, followed by mixed phases iron, chromium and nickel oxides that are in contact with the base alloy.

Oxide structure and corrosion products of coupons exposed to salts at 680°C were quite similar to observations made at 600°C. Sodium ferrite and iron oxide were both present on the outer surface, while mixed chromium and iron oxides were present beneath. Confirmation of this was determined using EMP and XRD in parallel (Figure 7 and 8). XRD found several additional peaks that are, as of this time, unidentified and may indicate some chemical reaction differences from the 600°C data.

Corrosion tended to proceed uniformly as surface corrosion for 347SS. No intergranular corrosion was identified specifically, though chromium depletion was observed along some grains on alloy 321SS. Figure 8 is one example of this behaviour. Migration of chromium along grain boundaries has been observed in molten chloride salt systems during the dealloying, which may suggest a similar behaviour here, though at a much lower rate [18].

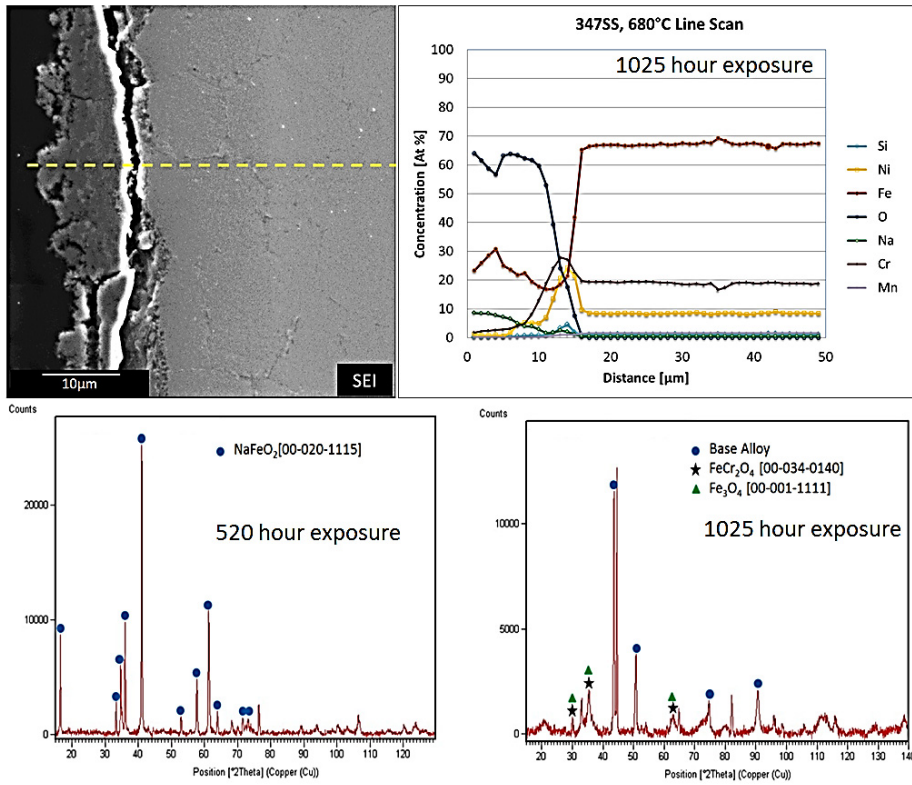


Figure 7: 347SS after 1025 hours exposure at 680°C. Phases of NaFeO<sub>2</sub> were detected with XRD after 520 hours (bottom left), with mixed oxide detected at 1025 hours (bottom right). Corrosion proceeded uniformly with no obvious grain boundary depletion of chromium.

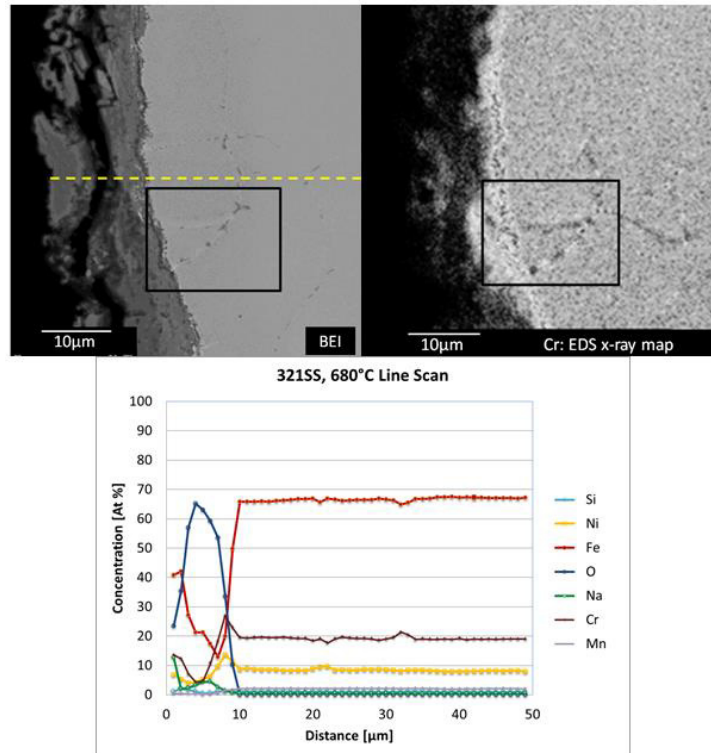


Figure 8: 321SS corrosion at 1025 hours at 680°C. Slight Cr depletion was observed along grain boundaries, indicated by EDS (top right).

#### 4. Conclusions

Corrosion rates for temperatures at 600°C and below were found to lose less than 16µm of metal per year. Under these conditions it was found that 347SS corroded at a rate of 30–40% less than 321SS. Spallation of corrosion products occurred at 600°C on 321SS and may be the reason for differing performance. At temperatures of 680°C corrosion rates among both alloys were found to be nearly the same, indicating that no protective barrier is being formed at these temperatures. Corrosion rates increased exponentially with temperature.

Oxidation mechanisms varied with temperature. Corrosion products observed at 500°C were primarily iron oxide on the outer surface with oxides of iron and chromium on the inner surface. Data at 600°C indicated that iron oxide and sodium ferrite were both present in the outer surface, while mixed oxides were again present near the base alloy and oxide interface. Corrosion at 680°C had similar morphology in relation to the 600°C with corrosion rates two orders of magnitude larger.

#### Acknowledgement

Sandia National Laboratories is a multi-program laboratory managed and operated by Sandia Corporation, a wholly owned subsidiary of Lockheed Martin Corporation, for the U.S. Department of Energy's National Nuclear Security Administration under contract DE-AC04-94AL85000, SAND 2013-2627 A

## References

1. *SunShot Initiative*. 2011 [cited 2011; Available from: <http://www1.eere.energy.gov/solar/sunshot/>].
2. Gary, J., C. Turchi, and N.P. Siegel, *CSP and the SunShot Initiative*, in *SolarPACES2011*, SolarPACES: Granada, Spain.
3. Stekli, J., *Thermal Energy Storage and the United States Department of Energy's SunShot Initiative*, in *SolarPACES2011*, SolarPACES: Granada, Spain.
4. Pacheco, J.E., et al., *Final test and evaluation results from the Solar Two project*, 2002, SAND2002-0120, Sandia National Laboratories, Albuquerque N. M.
5. Burgaleta, J.I., S. Arias, and D. Ramirez, *GEMASOLAR, The First Tower Thermosolar Commercial Plant with Molten Salt Storage*, in *SolarPACES 2011/2011*, SolarPACES: Granada, Spain.
6. Glatzmaier, G., *Materials for Sensible & Phase Change Thermal Storage*, in *Workshop on New Concepts and Materials for Thermal Energy Storage and Heat Transfer Fluids for CSP2011*, National Renewable Energy Laboratory: Golden, CO.
7. Siegel, N.P., *Thermal energy storage for solar power production*. Wiley Interdisciplinary Reviews: Energy and Environment, 2012. **1**(2): p. 119-131.
8. Jones, D.A., *Principles and prevention of corrosion*1996, Upper Saddle River, NJ: Prentice Hall.
9. Gill, D.D., et al., *DESIGN, FABRICATION AND TESTING OF AN APPARATUS FOR MATERIAL COMPATIBILITY TESTING IN NITRATE SALTS AT TEMPERATURES UP TO 700°C*, in *5th International Conference on Energy Sustainability2011*, ASME: Washington, DC, USA. p. 6.
10. Kruiuzenga, A.M., D.D. Gill, and M. LaFord, *Materials Corrosion of High Temperature Alloys Immersed in 600°C Binary Nitrate Salt*, 2013, SAND2013-2526, Sandia National Laboratories, Livermore C.A.
11. *Standard Practice for Preparing, Cleaning, and Evaluating Corrosion Test Specimens*, in *G1-032003*, ASTM International.
12. Bradshaw, R.W., *Corrosion of 304 stainless steel by molten NaNO<sub>3</sub>/KNO<sub>3</sub> [sodium nitrate/potassium nitrate] in a thermal convection loop*, 1980, SAND80-8856, Sandia National Laboratories, Livermore C. A.
13. Bradshaw, R.W., *THERMAL CONVECTION LOOP CORROSION TESTS OF 316SS AND IN800 IN MOLTEN NITRATE SALTS*, 1982, SAND82-8210, Sandia National Laboratories, Livermore C. A.
14. Bradshaw, R.W., *Oxidation and Chromium Depletion of Alloy 800 and 316SS by Molten NaNO<sub>3</sub>-KNO<sub>3</sub> at Temperatures Above 600 Degrees Centigrade*, 1987, SAND86-9009, Sandia National Laboratories, Livermore C. A.
15. Kerridge, D.H. and S.A. Tariq, *Molten sodium nitrite-potassium nitrite eutectic: the reactions of some compounds of chromium*. *Inorganica Chimica Acta*, 1969. **3**(0): p. 667-670.
16. Stott, F.H. and F.I. Wei, *High temperature oxidation of commercial austenitic stainless steels*. *Materials Science and Technology*, 1989. **5**(11): p. 1140-1147.
17. Bradshaw, R.W. and S.H. Goods, *Corrosion of alloys and metals by molten nitrates*, 2001, SAND2000-8727, Sandia National Laboratories, Livermore C. A.
18. Ambrosek, J., et al. *Corrosion studies of high temperature alloys in molten chloride salt*. in *2010 ANS Annual Meeting and Embedded Topical Meetings, June 13, 2010 - June 17, 2010*. 2010. San Diego, CA, United states: American Nuclear Society.